International Journal of Solids and Structures 48 (2011) 1034–1043

Contents lists available at ScienceDirect

International Journal of Solids and Structures

journal homepage: www.elsevier.com/locate/ijsolstr

Effect of multiple localized geometric imperfections on stability of thin axisymmetric cylindrical shells under axial compression

Limam Ali [a], El Bahaoui Jalal [b], Khamlichi Abdellatif [b,*], El Bakkali Larbi [b]

[a] Laboratory of Civil and Environmental Engineering, National Institute of Applied Sciences at Lyon, Albert Einstein Avenue, Villeurbanne 69662, France
[b] Modelling and Simulation of Mechanical Systems Laboratory, Faculty of Sciences at Tetouan, University Abdelmalek Essaadi, BP. 2121, M'hannech 93002, Tetouan, Morocco

ARTICLE INFO

Article history:
Received 31 March 2010
Received in revised form 25 August 2010
Available online 16 December 2010

Keywords:
Stability
Buckling
Shells
Finite element method
Localized imperfections
Analysis of variance

ABSTRACT

Stability of imperfect elastic cylindrical shells which are subjected to uniform axial compression is analyzed by using the finite element method. Multiple interacting localized axisymmetric initial geometric imperfections, having either triangular or wavelet shapes, were considered. The effect of a single localized geometric imperfection was analyzed in order to assess the most adverse configuration in terms of shell aspect ratios. Then two or three geometric imperfections of a given shape and which were uniformly distributed along the shell length were introduced to quantify their global effect on the shell buckling strength. It was shown that with two or three interacting geometric imperfections further reduction of the buckling load is obtained. In the ranges of parameters that were investigated, the imperfection wavelength was found to be the major factor influencing shell stability; it is followed by the imperfection amplitude, then by the interval distance separating the localized imperfections. In a wide range of parameters this last factor was recognized to have almost no effect on buckling stresses.

© 2010 Elsevier Ltd. All rights reserved.

1. Introduction

Thin shells are used in many fields of civil and mechanical engineering such as structural components: silos, tanks. Whatever the manufacturing process is used for these structures, the final geometry is never perfect. Geometrical defects disturb always the ideal desired nominal form of the assembled shell. Control and optimization of manufacturing processes of shells make it certainly possible today to decrease imperfections amplitudes, but they could never eliminate them completely. Even if, at first guess, the geometry seems to be perfect, precise measurements enable to detect always small geometric imperfections with magnitudes having in general the same order of scale than shell thickness.

During their service life, shell structures may be subjected to various kinds of loadings, such as axial compression, external/internal pressure, flexure or torsion. For cylindrical shells under axial compression, stability is an important design factor, (Gaylord and Gaylord, 1984; EN 1993-1-6, 2007; EN 1993-4-1, 2007). Calculation of the buckling load as it could be affected by the presence of various kinds of geometric imperfections constitutes an essential task. The European standard on shell buckling (ENV 1993-1-6, 2007) and the recent ECCS Recommendations on Stability of Shells (2008) require that when a geometrically nonlinear shell analysis with explicit representation of imperfections is used for design, a range of potentially damaging imperfection forms should be explored.

Several studies have been reported in the literature which deals with the effect of imperfections on buckling strength of thin shell structures. Arbocz and Babcock (1969) have studied experimentally buckling of cylindrical shells subjected to general imperfections. They have shown that huge reduction of the buckling critical load could be obtained. Koiter (1982) has given a review study about the effect of geometric imperfections on shell buckling strength. Other extensive investigations have considered the problem of shell buckling where analysis of the effects of distributed or localised imperfections on reduction of the buckling load has been performed (Yamaki, 1984; Arbocz, 1987; Bushnell, 1989 and Godoy, 1993). Kim and Kim (2002) have considered a generalised initial geometric imperfection having a modal superposition form. By using Donnell shell theory, (Donnell, 1934, 1976), they have studied the buckling strength of cylindrical shells and tanks subjected to axially compressive loads on soft or rigid foundations, they have found that the buckling load decreases significantly as the amplitude of initial geometric imperfection increases.

The above mentioned references have assessed, in all cases, that imperfections reduce drastically the buckling load of elastic cylindrical shells when subjected to axial compression. The obtained reduction depends on the nature of initial geometric imperfection that was considered. In general, reduction of the buckling load was

* Corresponding author.
E-mail addresses: ali.limam@insa-lyon.fr (L. Ali), jalalpc2@yahoo.fr (E.B. Jalal), khamlichi7@yahoo.es (K. Abdellatif), elbakkali@fst.ac.ma (E.B. Larbi).

0020-7683/$ - see front matter © 2010 Elsevier Ltd. All rights reserved.
doi:10.1016/j.ijsolstr.2010.12.007

found to be more severe in case of distributed imperfections than for localized ones.

Imperfections for which reduction of the buckling load attains a maximum are purely theoretical like for instance the sinusoidal imperfection in the form of the perfect shell linear axisymmetric eigenmode, known as the generalized Koiter imperfection, (Koiter, 1982), and might never be encountered in practice in case of real shells. Therefore, investigation has been motivated by the analysis of buckling in the presence of typical imperfections obtained from modal analysis of measured data or by considering realistic imperfection shapes such as those resulting from welding operations that are performed to assembly shell structures (Rotter, 2004). Steel silos and tanks are constructed from strakes that are welded together to assemble the complete shell structure. At circumferential welds localised geometric imperfections form. Measurements have revealed that mostly axisymmetric imperfections occur in these structures (Ding et al., 1996). Importance of the local axisymmetric imperfections occurring at these circumferential welds was first assessed by Bornscheuer et al. (1983a) and Bornscheuer and Haefner (1983b). Local axisymmetric depressions were previously recognized to constitute more realistic representations of initial geometric imperfections than full eigenmodes as was stated by Amazigo (1969), Hutchinson et al. (1971) and Amazigo and Budiansky (1972), however the first comprehensive study regarding the effect of these geometric imperfections was achieved by Rotter and Teng (1989) who have introduced the typical weld depression and studied its effect on the buckling strength. Other valuable studies which had addressed various aspects associated to weld-induced axisymmetric geometric imperfections can be found in Teng and Rotter (1992); Rotter and Zhang, 1990; Knödel et al. (1995), Guggenberger (1996), Knödel and Ummenhofer (1996), Knödel (1997), Berry and Rotter (1996), Holst et al. (2000), Berry et al. (2000), Schmidt and Winterstetter (2001), Pircher et al. (2001), Holst and Rotter (2002), Hübner et al. (2006), Ummenhofer (1998), Ummenhofer and Knödel (1996) and Ummenhofer et al. (1997).

Imperfections in welded shells take different forms as the profile of welding can vary from one shell to another, but a common feature of welds shapes is that they can be characterized by only two parameters: the defect amplitude and its width termed also wavelength. The axisymmetric weld depression that was introduced by Rotter and Teng (1989) is among the most easily recognizable such forms. Other forms were proposed after that. Mathon and Limam (2006) have compared the relative influence of several localised imperfections on reduction of the buckling load of shells subjected to axial compression or to flexure, and have shown that a triangular imperfection shape has the most severe effect on buckling strength.

Considering welds at different heights, Rotter (1996) was the first to study the interaction problem that could happen between them. Using a rigorous nonlinear analysis Rotter (1997) has studied this interaction in the case of the axisymmetric weld depression.

Emphasis will be done in the following on interaction effects that could result from multiple geometric weld imperfections. The localized initial imperfection geometry is assumed to have either a triangular shape or a wavelet shape. The shapes of these assumed imperfections are sharper than those of real imperfections encountered in axisymmetric shells, but some weld depressions could be closer to these shapes when fitted to analytical curves (Pircher et al., 2001). The main advantage of the theoretical shapes considered in this study is that they are more adequate to finite element modelling.

The two kind of localized geometric imperfections are considered either isolated or under situations where two or three imperfections having the previous forms are interacting. In this last case, the distance separating two adjacent defects is an additional parameter which might influence the shell buckling strength. One should add, to the three above mentioned factors, the classical shell aspect parameters: radius over thickness and length over radius.

In the subsequent, thin cylindrical axisymmetric shells made from homogeneous and isotropic elastic material are considered. They are assumed to deform under purely axisymmetric strain state when they are subjected to uniform axial compression. Investigation of the relative effect of the intervening five factors on reduction of the shell buckling load is performed by using the following methodology. At first, shell aspect ratios for which maximum effect on the buckling strength is obtained are determined. Then with this shell configuration being fixed, a parametric study is conducted by varying the three free remaining factors according to full factorial design of experiment tables. Analysis of variance is finally performed to determine the relative influence of factors.

2. Modelling of thin cylindrical shells having local defects

This study deals with the strength of imperfect cylindrical shells subject to uniform axial compression, for which the Eurocode (ENV 1993-1-6., 2007) terminology descriptions are used. According to this standard, three kind of buckling analyses are considered. These include the basic analysis termed Linear Bifurcation Analysis (LBA) which gives the reference buckling loads for any considered ideal problem conditions and provides mode shapes that could be used for expanding geometric imperfections. There is also, the geometrically nonlinear elastic analysis (GNA) which gives limit point loads for the perfect structure and enables to determine the importance of geometric nonlinearity for each considered loading case. To perform GNA analysis, it is of crucial importance that the eventuality of bifurcation occurrence should be examined at the end of any iteration in order to determine the nonlinear bifurcation load. The associated nonlinear buckling mode constitutes an additional imperfection form that could be considered in the analysis. The results of this work, which deals with the effect of initial geometric imperfections on shell buckling strength were derived by using geometrically nonlinear imperfection analysis (GNIA) with explicit representations of geometric imperfections.

In the context of elastic thin cylindrical shell buckling, a relevant finite element modelling based on Sanders–Koiter shell equations (Goldfeld, 2009) was developed by Combescure and Galletly (1999). This results in the software package called Stanlax which is based on an analytical expansion of circumferential variable contributions and finite element modelling of axial dependant quantities. This idea of cylindrical shell modelling was previously presented in works such as Bathe and Almeida (1980), Yan et al. (1999). Recently, Karamanos (2002) and Houliara and Karamanos (2010) have employed this methodology to perform analyses of bending instabilities occurring in thin shells.

In Stanlax modelling of buckling for imperfect cylindrical shells, the actual imperfect shell geometry is assumed to be obtained from the ideal cylindrical geometry by applying an initial small displacement defining the imperfection. The initial geometric imperfections are included in model formulation under the assumption that they yield only small perturbations to the ideal geometry. A detailed description of discretisation adopted by Stanlax software is given in the Appendix at the end of this paper. This Appendix presents also how computation of buckling is conducted.

Stanlax offers the possibility to perform either an LBA analysis through computing the linear Euler buckling mode for the perfect shell, Eq. (23), or a full non linear iterative computation of the buckling load according to Eurocode GNIA analysis, Eq. (21). For shells under axial compression, it was shown that Euler calculation of buckling by using the simplified Eq. (22) is sufficient since it

provides always results that are very close to those obtained by the more complete non linear analysis, Eq. (21), for which a lot of iterations are needed.

Stanlax software is used in the following in order to model the imperfect cylindrical axisymmetric shell having a given number of localized initial geometric imperfections.

The shell material is linear elastic having Young's modulus E and Poisson's coefficient υ. The geometric imperfections are assumed to be localized in the median zone of the shell length in positions that are sufficiently far from the shell extremities in order to avoid any significant interaction with boundary conditions. The selected boundary conditions are those corresponding to clamped shell ends.

As shown in Fig. 1, parameters t, L and R designate, respectively shell thickness, shell length and shell mean radius.

Let d and ℓ be respectively the geometric imperfection amplitude and the distance separating two contiguous imperfections. Let $\lambda_{cl} = \pi\sqrt{Rt}/(12(1-\upsilon^2))^{1/4} = 1.728\sqrt{Rt}$ be the half-wavelength of the classical axisymmetric buckling mode where υ is the Poisson's coefficient (Yamaki, 1984). The quantity λ_{cl} is termed here the reference wavelength and the following non-dimensional parameters describing the intervening five factors are introduced:

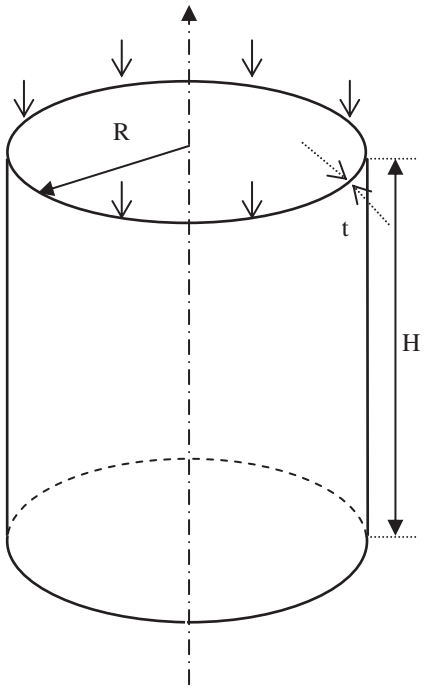

Fig. 1. Perfect shell geometry.

- R/t radius to thickness ratio;
- L/R length to radius ratio;
- d/t defect amplitude to shell thickness ratio;
- λ/λ_{cl} defect wavelength to reference wavelength ratio;
- ℓ/λ_{cl} interval length separating defects to reference wavelength ratio.

The first four dimensionless quantities were habitually introduced under these forms in previous literature dealing with local imperfections. As to the separation between imperfections, it is made dimensionless relative to the reference wavelength, because it is expected to capture in this way its significance in terms of the size of the buckles and their opportunities to interact.

The considered localized geometric imperfections have the two configurations shown in Fig. 2. Combinations of the interacting triangular geometric imperfections which are considered in the actual study have the configurations shown in Fig. 3. The same configurations are also adopted for the wavelet geometric imperfection.

Choosing imperfections that are directed inwards the shell radius, gives a total of six possible configurations. In addition to these, an outward triangular geometric imperfection was considered in order to assess the orientation effect on reduction of the buckling stress. It should be noted that Teng and Rotter (1992) have studied these two directions of imperfection for a different shape of axisymmetric imperfection in the form of the weld depression and have assessed that the inward defect is more severe that the outward one.

Stanlax software package enables for each combination of parameters to compute the shell buckling load when it is subjected to uniform axial compression P_x. Use is systematically made of shell element *Coque* and convergence assessment is performed in order to determine the optimal mesh size to be employed.

3. Parametric study of the shell buckling load as affected by localized geometric imperfections

The effect of a single localized geometric imperfection is investigated at first in order to determine the most adverse shell aspect parameters reducing the buckling load. This enables to fix parameters L/R and R/t, and to investigate the relative influence of the geometric imperfection for the remaining three parameters λ/λ_{cl}, d/t and ℓ/λ_{cl}.

3.1. Case of a single imperfection

Let's consider a single triangular geometric imperfection located at the mid height of the shell for which geometric and material properties are such that $R/t = 1500$, $L/R = 3$, $\lambda_{cl} = 6$ mm, $E = 70{,}000$ MPa and $\upsilon = 0.3$. In this case the classical buckling axial

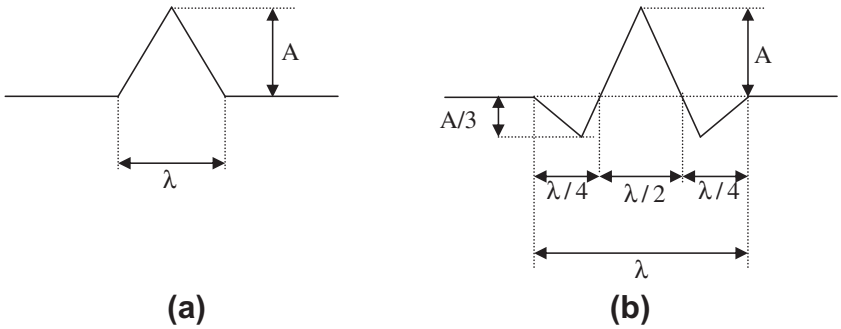

Fig. 2. Shapes of localized imperfections; (a) triangular geometric imperfection, (b) wavelet geometric imperfection.

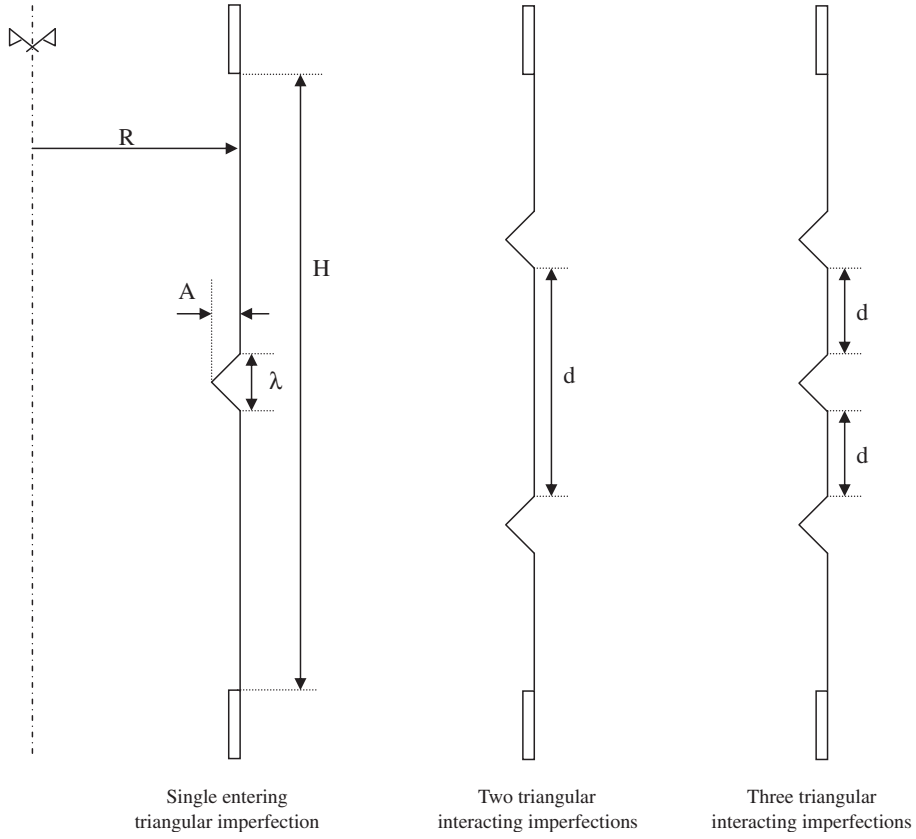

Fig. 3. Configurations of triangular localized geometric imperfections.

membrane stress is $\sigma_{cl} = 28.233$ MPa. When, the imperfection amplitude ratio is fixed at $d/t = 1$ and its wavelength ratio at $\lambda/\lambda_{cl} = 2.5$, Fig. 4 presents the evolution of the buckling stress ratio $\alpha = \sigma_{cr}/\sigma_{cl}$, with σ_{cr} the membrane axial stress at bifurcation and σ_{cl} the classical buckling membrane axial stress $\sigma_{cl} = \frac{E}{\sqrt{3(1-\upsilon^2)}} \times \frac{t}{R}$, as function of the number elements that are used in the finite element discretisation in the meridian axial direction and of the number of terms used in Fourier expansion in the circumferential direction.

Fig. 4 shows that a total number of 300 elements in the axial direction and a total number of 30 Fourier terms guarantee finite element model convergence. For all single or interacting imperfections, it was found that the previous numbers of elements and harmonics guarantee well convergence of the finite element model.

Fig. 5 gives a comparison between an inward triangular geometric imperfection and an outward one. The obtained results show that the first configuration is more critical than the second one. This was also verified for the other configurations associated to the two geometric imperfection shapes for all considered

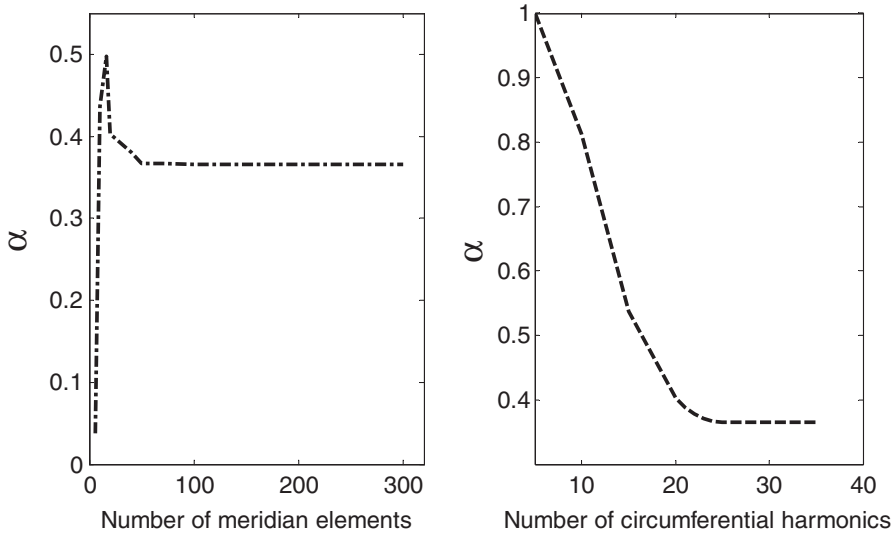

Fig. 4. Convergence study of the finite element model developed under Stanlax; single inward localized triangular imperfection.

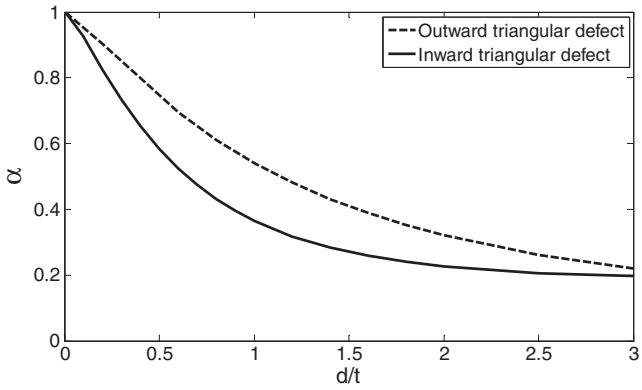

Fig. 5. Effect of triangular geometric imperfection orientation on the buckling load.

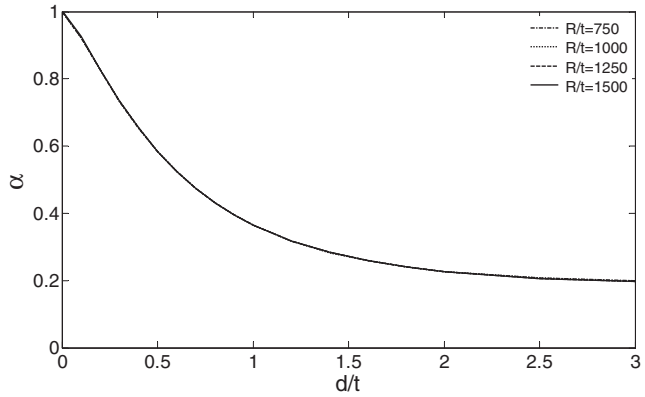

Fig. 7. Effect of shell aspect ratio on the buckling load reduction for $L/R = 3$.

numbers of interacting localized imperfections. This confirms the finding of Teng and Rotter (1992) to be valid also for the particular shapes of defects that were considered in this study.

A possible physical explanation for the inward imperfection to be more critical than the outward one may be seen in the fact that the radial resultant of the in-plane stresses in the curved shell has a deflection-dependant quadratic term which acts against formation of inward buckles and acts in favour of outward buckles. In case of outward imperfections of an axially compressed cylindrical shell, this would prevent many nonaxisymmetric buckling modes to develop and assists selecting axisymmetric patterns which have slightly higher critical stresses.

Inward oriented imperfections are more likely to develop as a consequence of welding process of shell strakes than the outward oriented ones. Since inward imperfections are also expected to be more damaging than the outward ones, the inward orientation will be the only one to be considered in the subsequent.

Fig. 6 gives the buckling stress ratio, for the case of a single inward triangular geometric imperfection, as function of wavelength and amplitude parameters when $L/R = 1$ and $R/t = 750$. It could be seen also from Fig. 6 that the wavelength $\lambda/\lambda_{cl} = 2.5$ yields the most adverse case since this curve is below those associated to $\lambda/\lambda_{cl} = 1$ and $\lambda/\lambda_{cl} = 4$ for amplitude ratio less than 2.3. $\lambda/\lambda_{cl} = 4$ is now the most adverse case when the amplitude ratio exceeds 2.3.

This is in accordance with the finding of Rotter (2004) who has demonstrated that the most adverse wavelength, as shown in Fig. 14 of that reference, depends on the amplitude of imperfection being studied, with the eigenmode wavelength critical only for the smallest amplitudes. The critical wavelength is growing and becoming steadily less precisely defined as the imperfection amplitude increases.

Fixing now $\lambda/\lambda_{cl} = 2.5$ and $L/R = 3$ for the case of a single inward triangular geometric imperfection, Fig. 7 gives the buckling stress ratio as function of shell aspect parameter R/t and the amplitude parameter d/t. These results show that for $L/R = 3$, the aspect ratio R/t dose not significantly affect the buckling strength while the amplitude ratio has a drastic effect on it.

Almost the same curves than those of Fig. 7, that are not shown here, were obtained for the single inward triangular defect when the shell aspect parameter is $L/R = 1$ and $\lambda/\lambda_{cl} = 2.5$, showing that there is only a small effect associated to parameter L/R. This can also be verified on Fig. 8, with shows also that the most adverse case is associated to $L/R = 3$.

Fixing $\lambda/\lambda_{cl} = 2.5$ and $R/t = 1500$ for the case of a single inward triangular geometric imperfection, Fig. 8 gives the buckling stress ratio as function of the shell aspect parameter L/R and the amplitude parameter d/t. The results show that there is only a small effect due to parameter L/R, while strong effect results from varying the amplitude parameter d/t.

Other results not given here have indicated that almost the same curves than those of Fig. 8 are obtained for the single inward triangular defect when using $\lambda/\lambda_{cl} = 2.5$ and $R/t = 750$, showing that the shell aspect ratio R/t has small influence on the buckling strength. Effect of parameter R/t is also confirmed to be small from Fig. 7, with the most adverse case being identified to be associated to $R/t = 1500$.

Regarding the effect of the inward wavelet local geometric imperfection on the buckling stress ratio as modified by parameters L/R, R/t and λ/λ_c, a similar parametric study than the one presented here above for the triangular defect was conducted. The same conclusions can be drawn.

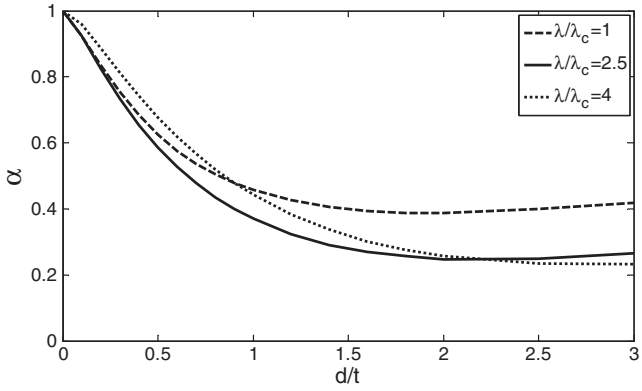

Fig. 6. Effect of wavelength α on the buckling load reduction for $R/t = 750$ and $L/R = 1$.

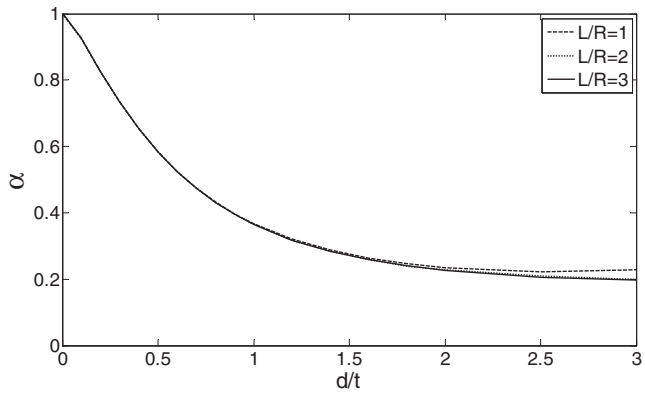

Fig. 8. Effect of shell aspect ratio on the buckling load reduction for $R/t = 1500$.

Table 1
Ranges of variation of geometric imperfection factors for both triangular and wavelet imperfections.

	λ/λ_{cl}	d/t	ℓ/λ_{cl}
Lower threshold	1.0	0.5	3.33
Higher threshold	3.0	2.5	16.67

3.2. Case of multiple interacting imperfections

The previous procedure was employed also when two or three interacting geometric imperfections are present and the same conclusions can be assessed again. So, the shell aspect parameters can be fixed at $L/R = 3$ and $R/t = 1500$. The influence of geometric imperfection parameters: λ/λ_{cl}, d/t and ℓ/λ_{cl} on the shell buckling load can now be straightforwardly investigated. This is performed in case of two or three interacting localized imperfections.

Table 1 lists levels of parameters that have been considered in the analysis of geometric imperfections under the coupling situations: lower threshold and higher threshold. Based on this table, parametric studies regarding the influence of two or three interacting geometric imperfections have been performed according to a design of experiment method using full factorial tables. A total set of 8 cases have been considered for each geometric imperfection shape and for each interacting configuration.

For the case $R/t = 1500$, $L/R = 3$, $\lambda/\lambda_{cl} = 2.5$ and for the two separation ratios $\ell/\lambda_{cl} = 3.33$ and $\ell/\lambda_{cl} = 16.67$ the obtained results in terms of the bifurcation stress ratio $\alpha = \sigma_{cr}/\sigma_{cl}$ versus parameter d/t are presented, respectively in Figs. 9 and 10 for triangular and wavelet geometric imperfections.

Considering the amplitude ratio $d/t = 2$ (with $R/t = 1500$, $L/R = 3$ and $\lambda/\lambda_{cl} = 2.5$) which corresponds to a rather big imperfection, Table 2 gives as function of ℓ/λ_{cl} a comparison between the obtained buckling stress ratio $\alpha = \sigma_{cr}/\sigma_{cl}$ for the different combina-

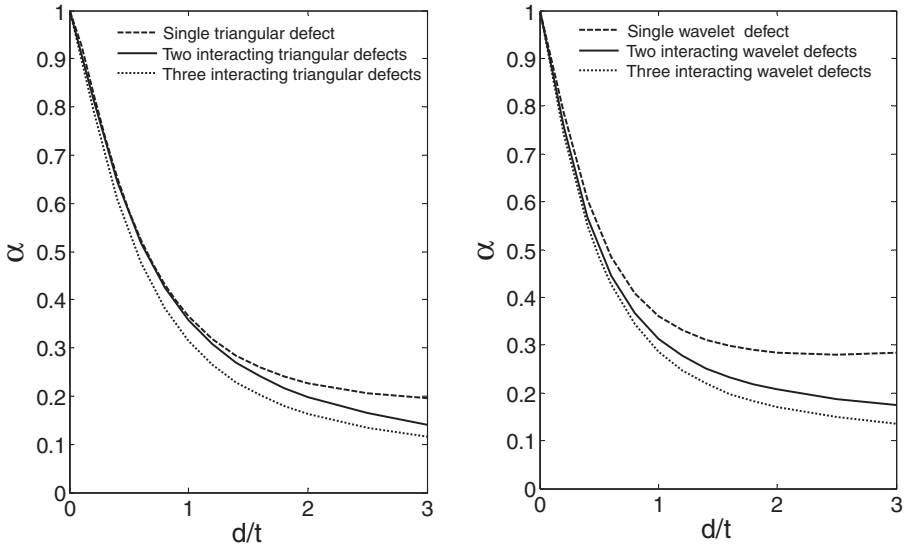

Fig. 9. Reduction of the buckling load as function of the localized imperfections configurations for $\ell/\lambda_{cl} = 3.33$; triangular geometric imperfections (left), wavelet geometric imperfections (right).

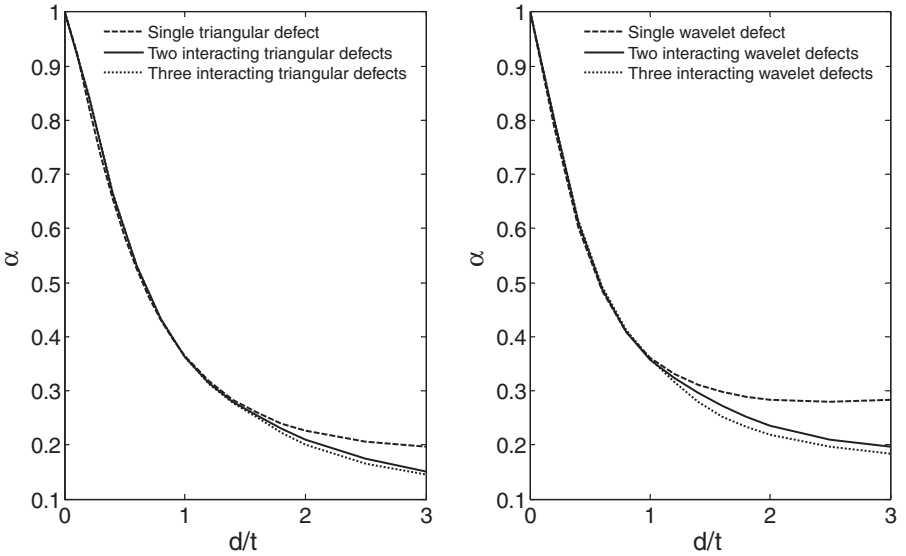

Fig. 10. Reduction of the buckling load as function of the localized imperfections configurations for $\ell/\lambda_{cl} = 16.67$; triangular geometric imperfections (left), wavelet geometric imperfections (right).

Table 2
Variations of the buckling stress ratio α as function of parameter ℓ/λ_{cl} for various cases of defects.

Shape of the defect	Triangular			Wavelet		
Number of defects	1	2	3	1	2	3
$\ell/\lambda_{cl} = 3.33$	0.226	0.175	0.165	0.283	0.258	0.195
$\ell/\lambda_{cl} = 16.67$	0.226	0.210	0.200	0.283	0.236	0.218

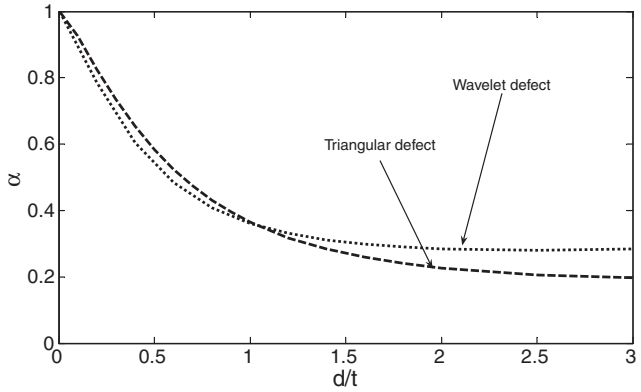

Fig. 11. Comparison of the buckling load as function of the single localized imperfection shape.

tions between the shape of initial geometric imperfection and the number of local imperfections on the shell structure.

The relative variation of the buckling stress ratio can reach the value of 45% for $d/t = 2$ and $\ell/\lambda_{cl} = 16.67$ in case of three wavelet imperfections. This variation can reach 67% for $d/t = 2$ and $\ell/\lambda_{cl} = 3.33$. However this variation is only about 1% for more realistic cases such as for example $d/t = 1$ and $\ell/\lambda_{cl} = 16.67$.

The contrast between the multiple defect and the single defect cases, as shown in Figs. 9 and 10, decreases when the amplitude ratio d/t decreases. This contrast is more pronounced when the imperfection amplitude is big. From Figs. 9 and 10, it can also be seen that the case where $\ell/\lambda_{cl} = 3.33$ yields greater variations as function of the number of defects while with $\ell/\lambda_{cl} = 16.67$ the variations are small, except for big imperfections.

Fig. 11 gives for $R/t = 1500$, $L/R = 3$ and $\lambda/\lambda_{cl} = 2.5$ a comparison of the buckling stress ratio computed for a single inward triangular imperfection and for a single inward wavelet one. One can notice that the triangular geometric imperfection yields the most severe reduction of the shell buckling load. But, if the geometric imperfection amplitude is controlled in such a way that it does not exceed the shell thickness, $d/t \leqslant 1$, than the wavelet defect yields the most important reduction of the shell buckling load.

3.3. The special effect of distance separating geometric imperfections

It is of particular interest to investigate how the interval distance ℓ separating the localized geometric imperfections which has the non-dimensional form ℓ/λ_{cl} may affect the shell buckling strength over a large range of parameter values. This may be of significant help to determine the optimal way of assembling shell strakes.

Fixing parameter $\lambda/\lambda_{cl} = 2.5$ and varying parameter d/t, Figs. 12 and 13 give, respectively in case of two and three inward triangular imperfections, the buckling stress ratio as function of parameter ℓ/λ_{cl}. It can be seen that parameter ℓ has not an equal effect on the buckling strength even if its global effect is rather limited. Small values of ℓ yield higher reduction of the buckling stress ratio, while for high values of separation distance ℓ the obtained buckling load is a little bit higher. Figs. 12 and 13 show that, for practical situations, parameter ℓ/λ_{cl} does not affect a lot the buckling stress.

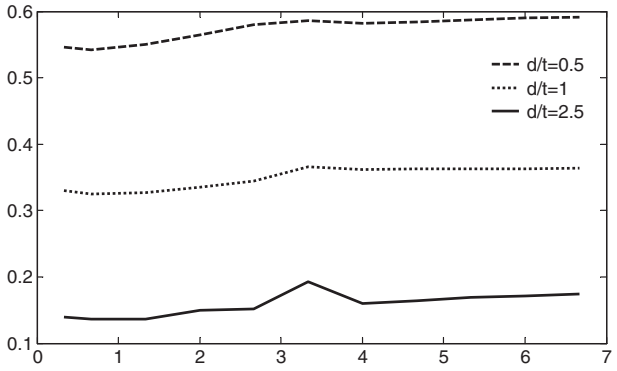

Fig. 12. Effect of parameter ℓ/λ_{cl} on the buckling load; two triangular geometric imperfections.

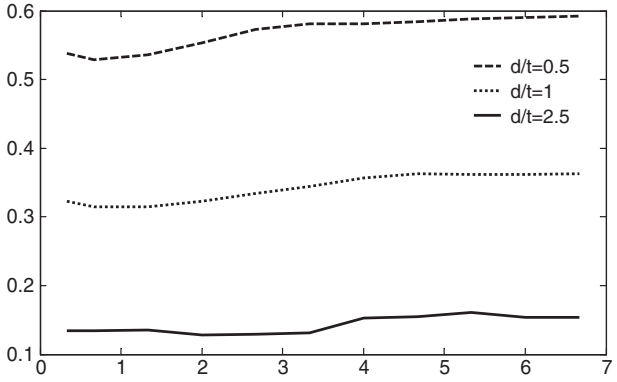

Fig. 13. Effect of parameter ℓ/λ_{cl} on the buckling load; three triangular geometric imperfections.

Table 3
p-Value statistics resulting from analysis of variance of the buckling stress ratio by means of the *F*-test.

	λ/λ_{cl}	d/t	ℓ/λ_{cl}
Two triangular imperfections	0.0004	0.0661	0.196
Three triangular imperfections	0.0437	0.1090	0.145
Two wavelet imperfections	0.0492	0.0113	0.493
Three wavelet imperfections	0.00005	0.0001	0.222

3.4. Analysis of variance

The observed variance on the buckling load can be partitioned into components due to the different sources of variations in terms of the three factors λ/λ_{cl}, d/t and ℓ/λ_{cr}. The F-test is conducted for that on the two-level 2^3 full factorial design, Table 1. The F-test is a statistical test in which the test statistics has an F-distribution (Fisher–Snedecor distribution) under the null hypothesis. The null hypothesis states here that there is no relationship between variation of a factor and that of the stress ratio.

Depending on the considered shape of geometric imperfection and on the number of localized initial geometric imperfections, analysis of variance, which was performed on the buckling load results obtained for the 8 combinations, has given when no interactions were considered between factors the p-values that are summarized in Table 3. The *p*-value is the probability of obtaining the test statistic at any realisation, assuming that the null hypothesis is true. The lower the *p*-value, the less likely the result is if the null hypothesis is true, and consequently the more significant the result is, in the sense of statistical significance.

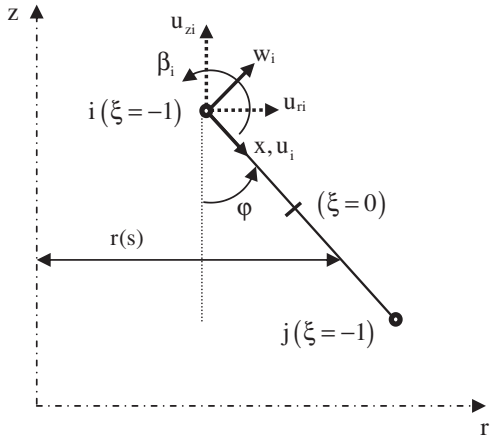

Fig. 14. Local displacements for a shell meridian segment element.

Table 3 shows that, for the ranges of parameters investigated here, the reduced wavelength parameter is the most significant factor. It is followed by the amplitude ratio and finally by the non-dimensional distance separating imperfections.

It should be noticed that the relative influence of factors in an analysis of variance depends a lot on their chosen rangers of variation. For other ranges than those specified in Table 1, the amplitude ratio might be the most dominant factor.

4. Conclusions

Numerical simulations based on the finite element method have been performed in order to quantify shell buckling load reduction in the presence of localized geometric imperfections. Elastic thin cylindrical shells subjected to axial compression and having one, two or three axisymmetric defects of inward triangular or wavelet shapes have been taken into account. A set of five factors intervening in the problem have been identified and their relative effect analysed.

After determining the most adverse case in terms of shell aspect ratios for a single geometric imperfection, a parametric study with regards to the remaining factors has been performed in case of multiple geometric imperfections according to full factorial design of experiment tables. Two or three imperfections regularly distributed along the shell length were investigated.

It has been shown in all cases that increasing the number of localized imperfections yield further reduction of the buckling load. This reduction is important and can reach 67% of the buckling stress in comparison with a single defect configuration if the imperfection amplitude is too big. However in common situations where the imperfection amplitude is small and the separation distance between defects is large, the influence of multiple local imperfections reduces to that of a single imperfection.

For a wide range of the separation distance between imperfections, almost no effect is observed as multiple defects make very little difference to the buckling stress.

For the ranges of parameters that were investigated, analysis of the relative influence of factors has shown that the imperfection wavelength has the maximum effect on the buckling strength. It is following by the imperfection amplitude and by the relative distance separating the multiple geometric imperfections.

Acknowledgement

The authors thank warmly Professor Alain Combescure from the National Institute of Applied Sciences at Lyon in France for having provided freely Stanlax software.

Appendix A. Computation of imperfect shell buckling and discretisation methodology adopted by Stanlax software in case of 2D elements

Geometry of a shell of revolution can be simply represented in one of its meridian planes. In the local cylindrical coordinates system denoted (r,z,θ), the continuous displacement of a point on the shell is denoted $[u_r \quad u_z \quad u_\theta]^t$ where $()^t$ designates the transpose operation.

The axisymmetric shell is considered in the following under the assumption that the initial geometry is imperfect with the imperfection amplitude remaining small so that the shell could be considered as quasi-axisymmetric, i.e. the imperfect geometry is obtained from the ideal geometry by applying a radial displacement field, $\bar{b}$. To model the shell buckling problem, a finite element formulation is used for the meridian axial coordinate, denoted x, and a Fourier expansion is used in the circumferential direction, θ. Finite element discretisation is performed on an augmented continuous displacement field which is assumed to be of the form $b = [u_r \quad u_z \quad u_\theta \quad \beta]^t$, where β is the rotation about the tangential axis, θ. The displacement field in the shell structure is expressed through the finite element and Fourier discretisations in terms of the vector of nodal displacements at each axial shell element which is denoted q.

Using a segment element having two nodes to approximate the local shell meridian geometry according to Marguerre theory, Fig. 14, and denoting (x,θ,n) the local shell coordinates system, the nodal displacement q_i is taken under the form $q = [u_i \quad v_i \quad w_i \quad \beta_i]^t$ where u_i is the axial meridian displacement, v_i the circumferential displacement, w_i the normal displacement and β_i the rotation about the tangential axis.

The nodal displacement for any given node i and any given circumferential position θ is assumed to be represented by a Fourier series such that

$$q_i = \sum_{n=0}^{Nh} q_{ci}^n \cos(n\theta) + \sum_{n=1}^{Nh} q_{si}^n \sin(n\theta) \tag{1}$$

where Nh is the number of considered harmonics, q_{ci}^n and q_{si}^n are the harmonic components of nodal displacement q_i associated respectively to cosine and to sine expansion terms.

The finite element interpolation is performed on the element $[i,j]$ according to

$$[u \quad v \quad w \quad \beta]^t = N(\xi)\begin{bmatrix} q_i \\ q_j \end{bmatrix} \tag{2}$$

with $N(\xi) = \left[\frac{1-\xi}{2} I_4 \quad \frac{1+\xi}{2} I_4\right]$, where I_4 is the identity matrix of rank 4.

Replacing the element nodal displacements by their Fourier expansions as given in (1) yield

$$[u \quad v \quad w \quad \beta]^t = \sum_{n=0}^{Nh} N_n(\xi)\begin{bmatrix} q_{ci}^n \\ q_{si}^n \\ q_{cj}^n \\ q_{sj}^n \end{bmatrix} = N_{Nh}(\xi) q \tag{3}$$

with

$$N_n(\xi,\varphi) = \left[\frac{1-\xi}{2}\cos(n\theta) I_4 \quad \frac{1-\xi}{2}\sin(n\theta) I_4 \quad \frac{1+\xi}{2}\cos(n\theta) I_4 \quad \times \frac{1+\xi}{2}\sin(n\theta) I_4\right]$$

and $N_{Nh}(\xi)$ is obtained by expanding all the Fourier modes.

As shown by Eq. (3), the total number of degrees of freedom per element is 16 (Nh + 1).

It is important that the initial imperfection displacement d should be decomposed in Fourier series in the same form than (1) with the same number of harmonics, such that

$$q_{d_i} = \sum_{n=0}^{\mathrm{Nh}} q^n_{\mathrm{dci}} \cos(n\theta) + \sum_{n=1}^{\mathrm{Nh}} q^n_{\mathrm{dsi}} \sin(n\theta) \tag{4}$$

which yields

$$[u_d \quad v_d \quad w_d \quad \beta_d]^t = \sum_{n=0}^{Nh} N_n(\xi) \begin{bmatrix} q^n_{\mathrm{dci}} \\ q^n_{\mathrm{dsi}} \\ q^n_{\mathrm{dcj}} \\ q^n_{\mathrm{dsj}} \end{bmatrix} = N_{\mathrm{Nh}}(\xi) q_d \tag{5}$$

Though Stanlax formulation can handle material nonlinearities, for clarity purposes restriction is made in the following to the case of linear elastic materials for which the stress–strain relationship takes the form

$$\sigma = H\varepsilon \tag{6}$$

where H is the matrix of elastic constants.

According to Sanders–Koiter theory for thin shells (Goldfeld, 2009), the strains-displacements relationships are given as

$$\begin{bmatrix} \varepsilon_x \\ \varepsilon_\theta \\ \varepsilon_{x\theta} \\ \chi_x \\ \chi_\theta \\ \chi_{x\theta} \end{bmatrix} = \underbrace{\begin{bmatrix} u_{,x} \\ \frac{v_{,\theta}}{r} + \frac{w\cos(\varphi)}{r} + \frac{u\sin(\varphi)}{r} \\ \frac{u_{,\theta}}{r} + v_{,x} - \frac{v\sin(\varphi)}{r} \\ \beta_{,x} \\ -\frac{w_{,\theta\theta}}{r^2} + \frac{\beta\sin(\varphi)}{r} + \frac{v_{,\theta}\cos(\varphi)}{r^2} \\ \frac{\beta_{,\theta}}{r} + \frac{w_{,\theta}\sin(\varphi)}{r^2} + \frac{v_{,x}\cos(\varphi)}{2r} - \frac{v\sin(2\varphi)}{4r^2} \end{bmatrix}}_{\varepsilon_L} + \frac{1}{2}\underbrace{\begin{bmatrix} \beta^2 \\ w^2_{,\theta} + \frac{v^2\cos^2(\varphi)}{2r^2} - \frac{vw_{,\theta}\cos(\varphi)}{r^2} \\ -\frac{\beta w_{,\theta}}{r} + \frac{v\beta\cos(\varphi)}{r} \\ 0 \\ 0 \\ 0 \end{bmatrix}}_{\varepsilon_Q} \tag{7}$$

These equations rewrite under the following form

$$\varepsilon = \varepsilon_L + \frac{1}{2}\varepsilon_Q = L(b) + \frac{1}{2}Q(b) \tag{8}$$

where subscripts L and Q indicate, respectively the linear part and the quadratic part,L is a linear functional and Q is a quadratic functional of displacement.

The bilinear functional associated to the quadratic functional Q is such that

$$Q(b_1, b_2) = \frac{1}{2}(Q(b_1 + b_2) - Q(b_1) - Q(b_2)) \tag{9}$$

If the displacement b is measured from the initial imperfect shell configuration, the total displacement as measured form the ideal axisymmetric reference configuration is $b_{\mathrm{imp}} = b + \bar{b}$. If there are no residual stresses associated with the initial displacement field, $\bar{b}$, then the strain consistent with the relation (6) may be expressed in the form

$$\varepsilon_{\mathrm{imp}}(b) = \varepsilon(b + \bar{b}) - \varepsilon(\bar{b}) = L(b) + \frac{1}{2}Q(b) + Q(b, \bar{b}) = \varepsilon(b) + Q(b, \bar{b}) \tag{10}$$

This shows that the imperfect strains $\varepsilon_{\mathrm{imp}}(b)$ are obtained by simply adding the quantity $Q(b, \bar{b})$ to the perfect strains $\varepsilon(b)$.

From Eqs. (7)–(10) one obtains the imperfect shell stain as

$$\varepsilon_{\mathrm{imp}}(b) = \begin{bmatrix} \varepsilon_{\mathrm{imp},x} \\ \varepsilon_{\mathrm{imp},\theta} \\ \varepsilon_{\mathrm{imp},x\theta} \\ \chi_{\mathrm{imp},x} \\ \chi_{\mathrm{imp},\theta} \\ \chi_{\mathrm{imp},x\theta} \end{bmatrix} = \varepsilon(b) + \begin{bmatrix} \beta\bar{\beta} \\ w_{,\theta}\bar{w}_{,\theta} + \frac{w_{,\theta}\bar{w}_{,\theta}\cos^2(\varphi)}{2r^2} - \frac{(v\bar{w}_{,\theta} + \bar{v}w_{,\theta})\cos(\varphi)}{r^2} \\ -\frac{\beta\bar{w}_{,\theta} + \bar{\beta}w_{,\theta}}{r} + \frac{(v\bar{\beta} + \bar{v}\beta)\cos(\varphi)}{r} \\ 0 \\ 0 \\ 0 \end{bmatrix} \tag{11}$$

Denoting by F the vector of forces, either volume forces or traction surfaces, which are applied on the shell structure, the equilibrium equation in variational form may be written as

$$\sigma \cdot \delta\varepsilon - F \cdot \delta b = 0 \tag{12}$$

where $\sigma \cdot \delta\varepsilon$ and $f \cdot \delta b$ denote, respectively, the internal virtual work of the stress σ through the strain variation $\delta\varepsilon$, and the external virtual work of the load F through the displacement variation δu, both integrated over the entire shell structure domain.

In buckling analysis proportional loading is considered, i.e. $F = \mu F_0$ where F_0 is a given constant loading and μ a scalar quantity. The imperfect displacement field $b_{\mathrm{imp}} = b + \bar{b}$ of the post-buckling equilibrium state can be written about the pre-buckling equilibrium state $b_{\mathrm{imp,cr}} = b_{\mathrm{cr}} + \bar{b}$, under the assumption of a single buckling mode, in the following form

$$b_{\mathrm{imp}} = b + \bar{b} = b_{\mathrm{cr}} + \bar{b} + \zeta v^* = b_{\mathrm{imp,cr}} + \zeta v^* \tag{13}$$

where b_{cr} is a nonlinear function of μ, while the buckling mode v^* is assumed independent of the perturbation parameter ζ which is assumed to be enough small.

Substitution of Eq. (13) in Eqs. (6) and (10) yields to the first order in ζ

$$\varepsilon_{\mathrm{imp}}(b) = \varepsilon_{\mathrm{imp,cr}} + \zeta\big(L(v^*) + Q(b_{\mathrm{cr}} + \bar{b}, v^*)\big) \tag{14}$$

$$\sigma_{\mathrm{imp}}(b) = \sigma_{\mathrm{imp,cr}} + \zeta H\big(L(v^*) + Q(b_{\mathrm{cr}} + \bar{b}, v^*)\big) \tag{15}$$

Using Eq. (11) and considering successively the pre-buckling and post-buckling states yield

$$\sigma \cdot \delta\varepsilon - \sigma_{\mathrm{cr}} \cdot \delta\varepsilon_{\mathrm{cr}} = 0 \tag{16}$$

Taking into account that from Eq. (14) we get $\delta\bar{\varepsilon} = \delta\bar{\varepsilon}_{\mathrm{cr}} + \zeta Q(\delta b_{\mathrm{cr}}, v^*)$, and substituting Eq. (15) in (16), the bifurcation condition is obtained as

$$\sigma_{\mathrm{imp,cr}} \cdot Q(\delta b_{\mathrm{cr}}, v^*) + H\big(L(v^*) + Q(b_{\mathrm{imp,cr}}, v^*)\big) \cdot \delta\bar{\varepsilon}_{\mathrm{cr}} = 0 \tag{17}$$

According to Eq. (10), the strain variation at the critical point can be obtained as

$$\delta\bar{\varepsilon}_{\mathrm{cr}} = L(\delta b_{\mathrm{cr}}) + Q(\delta b_{\mathrm{cr}}, b_{\mathrm{imp,cr}}) \tag{18}$$

Substitution of Eq. (18) in Eq. (17) yields the buckling condition

$$\begin{aligned} &\sigma_{\mathrm{imp,cr}} \cdot Q(\delta b_{\mathrm{cr}}, v^*) + HL(v^*) \cdot L(\delta b_{\mathrm{cr}}) + HQ(b_{\mathrm{imp,cr}}, v^*) \cdot L(\delta b_{\mathrm{cr}}) \\ &\quad + HL(v^*) \cdot Q(\delta b_{\mathrm{cr}}, b_{\mathrm{imp,cr}}) + HQ(b_{\mathrm{imp,cr}}, v^*) \\ &\quad \cdot Q(\delta b_{\mathrm{cr}}, b_{\mathrm{imp,cr}}) = 0 \end{aligned} \tag{19}$$

In the finite element implementation, an interpolation of displacement is considered as $b = Nq$ where N is the matrix of shape functions. Substituting this interpolation in Eq. (19) and because variations are arbitrary, one arrives at the disretized buckling condition

$$\begin{aligned} &B^t_{\mathrm{NL}}(v^*)\sigma_{\mathrm{imp,cr}} + B^t_L H B_L v^* + B^t_{\mathrm{NL}}(q_{\mathrm{imp,cr}}) H B_L v^* + B^t_L H B_{\mathrm{NL}}(q_{\mathrm{imp,cr}}) v^* \\ &\quad + B^t_{\mathrm{NL}}(q_{\mathrm{imp,cr}}) H B_{\mathrm{NL}}(q_{\mathrm{imp,cr}}) v^* = 0 \end{aligned} \tag{20}$$

where $q_{\mathrm{imp,cr}} = q_{\mathrm{cr}} + \bar{q}$, B_L and B_{NL} are matrices defined at each integration point and correspond, respectively to L and Q functionals in Eq. (8). They have the form $B_L = LN$ and $B_{\mathrm{NL}}(q) = q^t G(N)$, where G is a geometric operator acting on the shape functions N.

In Stanlax, integrations over the thickness and over the circumferential direction domains are performed analytically; the meridian axial integration is performed numerically by using only one Gauss point.

Now for the buckling problem we can rewrite Eq. (20) after element level integration and assembly process as

$$[K_\sigma + K_L + K_{NL}(q + \bar{q})]V^* = 0 \tag{21}$$

where K_σ, K_L, and K_{NL} are initial displacement, the linear and nonlinear geometric stiffness matrices.

The strategy for solving Eq. (21) consists in incrementing the load λF_0 till for the first time Eq. (21) admits a non trivial solution $V^* \neq 0$.

If displacements remain small, than the geometric stiffness matrix could be approximated to $K_{NL}(\bar{q})$ yielding to the pseudo Euler buckling equation

$$[K_\sigma + K_L + K_{NL}(\bar{q})]V^* = 0 \tag{22}$$

The buckling problem reduces in this case to a one step eigenvalue problem for which solution can be obtained very quickly.

According to the Eurocode (ENV 1993-1-6, 2007) terminology, the LBA analysis may be performed by assuming in Eq. (22) $\bar{q} = 0$ such that

$$[K_\sigma + K_L]V^* = 0 \tag{23}$$

while Eq. (21) can be used to perform a GNIA analysis and GNA analysis corresponds to Eq. (21), but with $\bar{q} = 0$.

References

Amazigo, J.C., 1969. Buckling under axial compression of long cylindrical shells with random axisymmetric imperfections. Quarterly of Applied Mathematics 26, 537–566.

Amazigo, J.C., Budiansky, B., 1972. Asymptotic formulas for the buckling stresses of axially compressed cylinders with localized or random axisymmetric imperfections. Journal of Applied Mechanics 93, 179–184.

Arbocz, J., 1987. Post-buckling behaviour of structures, numerical techniques for more complicated structures. Buckling and Postbuckling of Structures. Springer-Verlag, Berlin.

Arbocz, J., Babcock, C.D., 1969. The effect of general imperfections on the buckling of cylindrical shells. ASME Journal of Applied Mechanics, 36 28–38.

Bathe, K.-J., Almeida, C.A., 1980. A simple and effective pipe elbow element- linear analysis. ASME Journal of Applied Mechanics 47, 93–100.

Berry, P.A., Rotter, J.M., 1996. Partial axisymmetric imperfections and their effect on the buckling strength of axially compressed cylinders. In: Proceedings International Workshop on Imperfections in Metal Silos: Measurement, Characterisation and Strength Analysis, CA-Silo, Lyon, France, 19 April, pp. 35–48.

Berry, P.A., Rotter, J.M., Bridge, R.Q., 2000. Compression tests on cylinders with circumferential weld depressions. Journal of Engineering Mechanics, ASCE 126 (4), 405–413.

Bornscheuer, F.W., Haefner, L., 1983b. The influence of an imperfect circumferential weld on the buckling strength of axially loaded circular cylindrical shells. Prelim. Report. In: 3rd International Colloquium on Stability of Metal Structures, Paris, pp. 407–414.

Bornscheuer, F.W., Haefner, L., Ramm, E., 1983a. Zur Stabilitat eines Kreiszylinders mit einer Rundschweissnaht unter Axialbelastung. Der Stahlbau 52 (10), 313–318.

Bushnell, D., 1989. Computerized analysis of shells. Mechanics of Elastic Stability. Kluwer Academic Publishers, Dordrecht, Boston, London.

Combescure, A., Galletly, G.D., 1999. Plastic buckling of complete toroidal shells of elliptical cross-section subjected to internal pressure. Thin-Walled Structures 34 (2), 135–146.

Ding, X., Coleman, R., Rotter, J.M., 1996. Technique for precise measurement of large-scale silos and tanks. Journal of Surveying Engineering 122, 15–25.

Donnell, L.H., 1934. A new theory for the buckling of thin cylinders under axial compression and bending. Transactions of ASME 56, 795–806.

Donnell, L.H., 1976. Beams, Plates and Shells. McGraw Hill, New York.

ECCS, 2008. European Recommendations for Steel Construction: Buckling of Shells, fifth edition, In: Rotter, J.M., Schmidt, H. (Eds.), European Convention for Constructional Steelwork, Brussels, 384 pp.

EN 1993-1-6, 2007. Eurocode 3: Design of steel structures, Part 1.6: General rules – Strength and stability of shell structures, Eurocode 3 Part 1.6, CEN, Brussels.

EN 1993-4-1, 2007. Eurocode 3: Design of steel structures, Part 4.1: Silos, Eurocode 3 Part 4.1, CEN, Brussels.

Gaylord, E.H., Gaylord, C.N., 1984. Design of Steel Bins for Storage of Bulk Solids. Prentice Hall.

Godoy, L.A., 1993. On loads equivalent to geometrical imperfections in shells. Journal of Engineering Mechanics, ASCE 119, 186–190.

Goldfeld, Y., 2009. An alternative formulation in linear bifurcation analysis of laminated shells. Thin-Walled Structures 47, 44–52.

Guggenberger, W., 1996. Effect of geometric imperfections taking into account the fabrication process and consistent residual stress fields of cylinders under local axial loads. In: Proceedings of International Workshop on Imperfections in Metal Silos: Measurement, Characterisation and Strength Analysis, CA-Silo, Lyon, France, 19 April, pp. 217–228.

Holst, J.M.F.G., Rotter, J.M., 2002. Buckling strength of cylinders with a consistent residual stress state. In: Proceedings of Third International Conference on Advances in Steel Structures, ICASS'02, Hong Kong, December 2002, vol. II, pp. 729–736.

Holst, J.M.F.G., Rotter, J.M., Calladine, C.R., 2000. Imperfections and buckling in cylindrical shells with consistent residual stresses. Journal of Constructional Steel Research 54, 265–282.

Houliara, S., Karamanos, S.A., 2010. Stability of long transversely-isotropic elastic cylinders under bending. International Journal of Solids and Structures 47 (1), 10–24.

Hübner, A., Teng, J.G., Saal, H., 2006. Buckling behaviour of large steel cylinders with patterned welds. International Journal of Pressure Vessels and Piping 83, 13–26.

Hutchinson, J.W., Tennyson, R.C., Muggeridge, D.B., 1971. Effect of a local axisymmetric imperfection on the buckling of a cylindrical shell under axial compression. AIAA Journal 9, 48–52.

Karamanos, S.A., 2002. Bending Instabilities of Elastic Tubes. International Journal of Solids and Structures 39 (8), 2059–2085.

Kim, S.E., Kim, C.S., 2002. Buckling strength of the cylindrical shell and tank subjected to axially compressive loads. Thin-Walled Structures 40, 329–353.

Knödel, P., 1997. A simple model for assessing the buckling strength of silos. In: Proceedings of the International Conference on Carrying Capacity of Steel Shell Structures, Brno, 1–3 October 1997, pp. 85–90.

Knödel, P., Ummenhofer, T., 1996. Substitute imperfections for the prediction of buckling loads in shell design. In: Proceedings of the International Workshop on Imperfections in Metal Silos: Measurement, Characterisation and Strength Analysis, CA-Silo, Lyon, France, 19 April 1996, pp. 87–102.

Knödel, P., Ummenhofer, T., Schulz, U., 1995. On the modelling of different types of imperfections in silo shells. Thin-Walled Structures 23, 283–293.

Koiter, W.T., 1982. The application of the initial post-buckling analysis to shells. In: Buckling of Shells, Proceedings of a State-of-the-Art Colloquium. Springer-Verlag, Berlin, Heidelberg, New York, pp. 63–77.

Mathon, C., Limam, A., 2006. Experimental collapse of thin cylindrical shells submitted to internal pressure and pure bending. Thin-Walled Structures 44, 39–50.

Pircher, M., Berry, P.A., Ding, X., Bridge, R.Q., 2001. shape of circumferential weld-induced imperfections in thin-walled steel silos and tanks. Thin-Walled Structures 39, 999–1014.

Rotter, J.M., 1996. Elastic plastic buckling and collapse in internally pressurised axially compressed silo cylinders with measured axisymmetric imperfections: interactions between imperfections, residual stresses and collapse. In: Proceedings of the International Workshop on Imperfections in Metal Silos: Measurement, Characterisation and Strength Analysis, CA-Silo, Lyon, France, 19 April 1996, pp. 119–140.

Rotter, J.M., 1997. Design standards and calculations for imperfect pressurised axially compressed cylinders. In: Proceedings of the International Conference on Carrying Capacity of Steel Shell Structures, Brno, 1–3 October 1997, pp. 354–360.

Rotter, J.M., 2004. Buckling of cylindrical shells under axial compression. In: Buckling of Thin Metal Shells. Spon, London, pp. 42–87.

Rotter, J.M., Teng, J.G., 1989. Elastic stability of cylindrical shells with weld depressions. Journal of Structural Engineering 115 (5), 1244–1263.

Rotter, J.M., Zhang, Q., 1990. Elastic buckling of imperfect cylinders containing granular solids. Journal of Structural Engineering, ASCE 116 (8), 2253–2271.

Schmidt, H. and Winterstetter, T.A., 2001. Substitute geometrical imperfections for the numerical buckling assessment of cylindrical shells under combined loading. In: Proceedings of the European Mechanics Conference: Euromech 424, Rolduc-Kerkrade, Germany, 3–5 September 2001, pp. 82–84.

Teng, J.G., Rotter, J.M., 1992. Buckling of pressurized axisymmetrically imperfect cylinders under axial loads. Journal of Engineering Mechanics, ASCE 118 (2), 229–247.

Ummenhofer, T., 1998. Finite element analysis of the stress state and stability of metal silo structures. In: Brown, C.J., Nielsen, J. (Eds.), Silos: Fundamentals of Theory, Behaviour and Design. E & FN Spon, London, pp. 452–460 (Chapter 22).

Ummenhofer, T., Knödel, P., 1996. Typical imperfections of steel silo shells in Civil Engineering. In: Proceedings of the International Workshop on Imperfections in Metal Silos: Measurement, Characterisation and Strength Analysis, CA-Silo, Lyon, France, 19 April 1996, pp. 103–118.

Ummenhofer, T., Peil, U., Schulz, U., 1997. A rigorous model for assessing the buckling strength of silos. In: Proceedings of the International Conference on Carrying Capacity of Steel Shell Structures, Brno, 1–3 October 1997, pp. 91–97.

Yamaki, N., 1984. Elastic stability of circular cylindrical shells. Applied Mathematics and Mechanics 27.

Yan, A.M., Jospin, R.J., Nguyen, D.H., 1999. An enhanced pipe elbow element – Application in plastic limit analysis of pipe structures. International Journal For Numerical Methods in Engineering 46, 409–431.